



Contents lists available at ScienceDirect

## Journal of Cardiovascular Computed Tomography

journal homepage: [www.JournalofCardiovascularCT.com](http://www.JournalofCardiovascularCT.com)

Review article

## CT imaging with ultra-high-resolution: Opportunities for cardiovascular imaging in clinical practice

Joanne D. Schuijf<sup>a</sup>, João A.C. Lima<sup>b</sup>, Kirsten L. Boedeker<sup>c</sup>, Hidenobu Takagi<sup>d,e,f</sup>, Ryoichi Tanaka<sup>d</sup>, Kunihiro Yoshioka<sup>d</sup>, Armin Arbab-Zadeh<sup>b,\*</sup><sup>a</sup> Global RDC, Canon Medical Systems Europe BV, Zoetermeer, the Netherlands<sup>b</sup> Division of Cardiology, Department of Medicine, Johns Hopkins University School of Medicine, Baltimore, MD, USA<sup>c</sup> Canon Medical Systems, Otawara, Japan<sup>d</sup> Department of Radiology, Iwate Medical University Hospital, Morioka, Japan<sup>e</sup> Department of Radiology, The University of British Columbia, St. Paul's Hospital, BC, Canada<sup>f</sup> Department of Diagnostic Radiology, Tohoku University Hospital, Sendai, Japan

## ARTICLE INFO

## Keywords:

Computed tomography  
 Coronary computed tomography angiography  
 Coronary artery disease  
 Vascular imaging  
 Ultra-high resolution CT

## ABSTRACT

Cardiovascular computed tomography (CT) angiography has become an established alternative to invasive catheter angiography. However, imaging artifacts due to partial volume effects with current systems hinder accurate evaluation of calcified or stented segments. Increased spatial resolution may allow to overcome these barriers to precise delineation of vascular disease. Recent developments in CT hardware and reconstruction have enabled CT angiography with ultra-high spatial resolution (UHRCT). In this review we aim to describe the methods to achieve greater spatial resolution in CT that are either in clinical or preclinical stage. In addition, we provide an overview of the available clinical evidence including diagnostic accuracy studies supporting improved vascular assessment with this technology. The benefits that can be gleaned from the initial experiences with UHRCT are promising. Using UHRCT, more patients may receive non-invasive characterization of coronary atherosclerosis by overcoming the limitations of current CT spatial resolution in visualizing and quantifying calcified, stented or small diameter segments. UHRCT may potentially impact existing management pathways as well as contribute to better understanding of the underlying pathophysiology of both macro- and microvascular disease.

## 1. Introduction

During the last decades, cardiovascular computed tomography (CT) has matured into a routine imaging tool for many applications in cardiovascular medicine. The technique has entered major societal guidelines.<sup>1,2</sup> In the past, the development focus of multidetector row CT has typically been on temporal resolution by increasing the speed of acquisition and motion artifact control through increasing the number of detector rows to achieve whole organ imaging without the need for translational motion. These successful efforts were followed by marked reduction in radiation dose. At present, new system designs are being introduced to tackle the next challenge of providing much greater

spatial resolution from the 0.400–0.500 mm to the 0.150–0.200 mm range.<sup>3</sup>

One area of particular interest is cardiovascular imaging, an application for which improved spatial resolution could be particularly beneficial. Whereas for visualization of major epicardial coronary arteries CT angiography has become an established alternative to invasive coronary angiography (ICA), imaging artifacts due to partial volume effects hinder accurate evaluation of smaller and calcified epicardial arterial segments with current systems.<sup>4–6</sup> Similarly, quantification of plaque progression and regression, and clear intra-luminal visualization of stented vascular segments remain challenging and often clinically insufficient at present.<sup>4–6</sup> The need for greater delineation of vascular disease non-invasively has

**Abbreviations:** CABG, coronary artery bypass grafting; CAD, coronary artery disease; CT, computed tomography; ICA, invasive coronary angiography; NR, normal resolution; OMT, optimal medical therapy; PCI, percutaneous coronary intervention; PCCT, photon-counting CT; SHR, super-high-resolution; UHRCT, ultra-high spatial resolution CT.

\* Corresponding author. Department of Medicine-Division of Cardiology, 600 N. Wolfe Street, Halsted 562, Baltimore, MD, 21287-0025, USA.

E-mail address: [azadeh1@jhmi.edu](mailto:azadeh1@jhmi.edu) (A. Arbab-Zadeh).

<https://doi.org/10.1016/j.jcct.2022.02.003>

Received 14 September 2021; Received in revised form 3 February 2022; Accepted 5 February 2022

Available online xxx

1934-5925/© 2022 The Authors. Published by Elsevier Inc. on behalf of Society of Cardiovascular Computed Tomography. This is an open access article under the CC

BY license (<http://creativecommons.org/licenses/by/4.0/>).

fueled interest in further increasing CT spatial resolution. Indeed, achieving the resolution of invasive angiographic evaluation could provide new opportunities for non-invasive diagnosis, monitoring and even treatment planning of patients with suspected or confirmed coronary artery disease (CAD) and other vascular pathologies. Moreover, accurate evaluation of even smaller segments like myocardial perforating vessels and arterioles of diameters below the 0.400 mm threshold of current CT technology could improve our understanding of microvascular disease underlying angina pectoris and heart failure with preserved ejection fraction. In this review we aim to describe the methods to achieve greater spatial resolution using CT, and the currently available evidence for visualization and assessment of vascular structures with this technology. Finally, we discuss the potential impact higher spatial resolution may have on diagnostic pathways and understanding of the underlying pathophysiology of both macro- and microvascular disease.

## 2. Current methods and challenges to achieve ultra-high spatial resolution CT

In CT, spatial resolution depends on several hardware and data acquisition features including detector element size, X-ray focal spot size, and detector response function, in addition to the image reconstruction algorithm used. Ultra-high spatial resolution (UHR) imaging has inherent challenges such as increased susceptibility to motion artifacts and image noise. Therefore, greater demands are placed on gantry and couch design to improve mechanical stability and reduce vibration when compared to conventional CT systems. Smaller detector pixels come with the trade-off of either increased image noise, or increased radiation dose to maintain similar levels of image noise. As such, noise reduction strategies become crucial. Finally, imaging with increased spatial resolution also brings considerable challenges in data management. The substantial increase in image data volume requires greater workstation post-processing power, larger storage size for image archival, and greater network speed for image transfer.

Photon-counting CT (PCCT) is a promising approach that is currently pursued by all major CT manufacturers. PCCT is based on the powerful concept of measuring each penetrating photon individually for the ultimate purpose of acquiring multi-energy images to differentiate and quantify structural material composition.<sup>7-9</sup> However, the technology can also be applied to acquire images with increased spatial resolution. Recently, the first PCCT system has been released for commercial use. This system is a dual-source system with cadmium telluride-based photon-counting detectors and has two acquisition modes, standard multi-energy mode and UHR mode.<sup>10</sup> In UHR mode, a 0.125 mm in-plane resolution can theoretically be achieved, with  $120 \times 0.2$  mm (24 mm) z-coverage and  $1024 \times 1024$  matrix reconstruction, corresponding in optimal conditions to 36 lp/cm at the Modulation Transfer Function (MTF)10%.<sup>11</sup> At present, cardiac acquisitions are done in the standard multi-energy mode using a z-coverage of 57.6 mm obtained through a  $144 \times 0.4$  mm detector row configuration.<sup>11</sup> Research exploring the potential of this PCCT system in UHR mode for cardiac has been performed using earlier prototype systems consisting of one photon-counting detector. With these prototypes, UHR mode was generated by grouping detector elements into a  $2 \times 2$  formation rather than the  $4 \times 4$  formation for conventional resolution, resulting in a  $0.25$  mm  $\times$   $0.25$  mm spatial resolution at the isocentre.<sup>7,9</sup> In a feasibility study, Pourmorteza et al. showed a doubling of spatial resolution with this 0.25 mm slice acquisition strategy albeit with 75% noise increase, when compared with the standard dose-matched 0.5-mm slice acquisition mode.<sup>12</sup> Noise could be mitigated by “downgrading” the reconstruction resolution to 0.5 mm.<sup>12</sup> Another clinical prototype consists of a  $64 \times 0.275$  mm detector row system.<sup>13</sup> Finally, in addition to cadmium-telluride or cadmium-zinc-telluride also silicon-based PCCT detectors are explored.<sup>14</sup> Important technological challenges for PCCT include detector related artifacts such as cross-talk and pulse pile up effects.<sup>3,7</sup> The associated high costs of producing PCCT detectors may limit

routine clinical use on a wide scale in the near term as well.<sup>7</sup> The potential of PCCT for cardiac applications in particular has been recently reviewed by Sandfort et al.,<sup>8</sup> while more data on systems, either in research or clinical use, are expected to emerge soon.

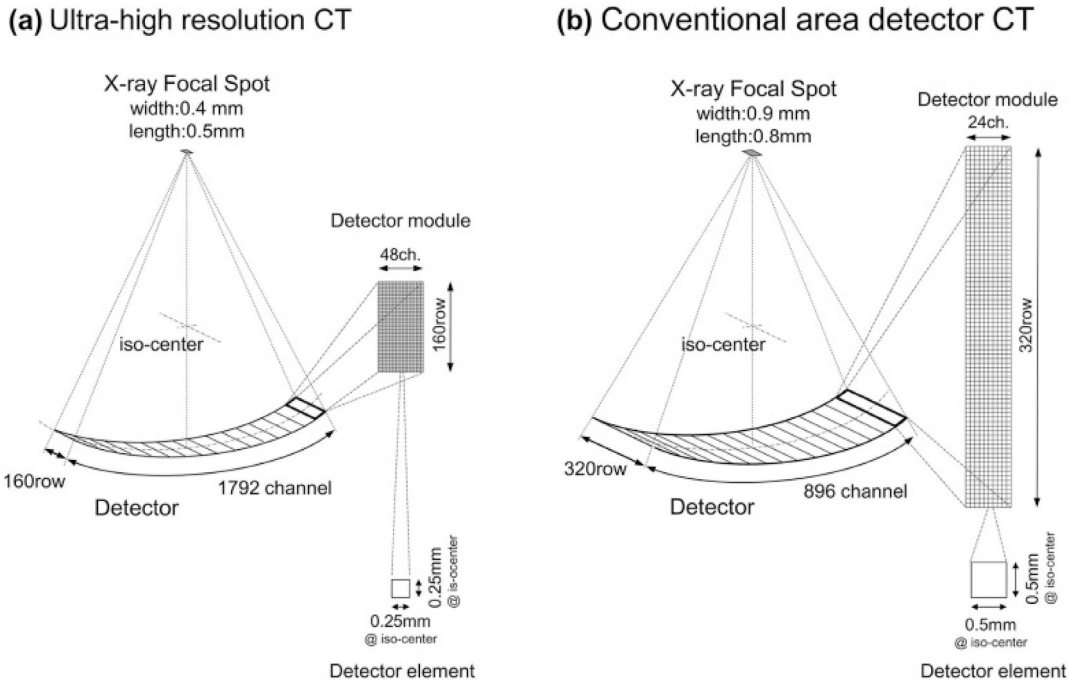
A method that has been available for clinical use for several years is a dedicated UHR CT scanner based on conventional detector design.<sup>15</sup> This system is a 160-row multi-detector row scanner with superfine detector elements providing an effective detector element size of  $0.25$  mm  $\times$   $0.25$  mm at the isocenter, corresponding in optimal conditions to an MTF10% of 41 lp/cm.<sup>15</sup> An adaptive focal spot X-ray tube is available with a minimum focus size as small as  $0.4$  mm  $\times$   $0.5$  mm. In addition to the conventional  $512 \times 512$  matrix, high-resolution acquisitions can be reconstructed with  $1024 \times 1024$ , and  $2048 \times 2048$  matrix sizes, providing greater detail.<sup>16,17</sup> The system includes the option to scan in several modes: super-high-resolution (SHR) mode which uses  $0.25$  mm (at the iso-center) detector elements in the in-plane and longitudinal directions, high-resolution HR mode which bins two detector elements in the longitudinal direction and current normal resolution (NR) mode which bins detector elements  $2 \times 2$ , resulting in a detector element-size equivalent to that of a current generation CT system. A detailed description of the system and the modifications as compared to a conventional high-end scanner to enable true UHR imaging is provided in Fig. 1.

In clinical practice, limitations of the current system pertinent for cardiac imaging include the decreased detector coverage (40 mm) as compared to wide volume systems. As for other high-resolution CT approaches, images obtained with high resolution modes are affected by increased noise. While doubling the spatial resolution, the low-contrast detectability of the high-resolution modes obtained with UHRCT was shown to be lower than that of standard CT at the same radiation dose; an extra dose of 23% was needed to obtain the same low-contrast detectability.<sup>15</sup> Dedicated deep learning reconstruction algorithms have been developed for noise reduction that allow dose neutral high-resolution imaging and maintain image quality in patients with high body mass index.<sup>18-20</sup> An example of noise reduction when using a deep learning reconstruction algorithm specifically developed for cardiac UHRCT is provided in Fig. 2. This deep learning reconstruction algorithm is trained on high dose images reconstructed with Model-Based Iterative Reconstruction (MBIR). MBIR takes the relevant system and anatomical models into account during reconstruction. In addition, the MBIR used to create the training data used a large number of iterations, as reconstruction time in a factory setting is not prohibitive, in order to optimize the image quality of the training target data. The high quality training data is then corrupted with added noise used as input data. The deep learning neural network learns to de-noise input data while maintaining spatial resolution by minimizing the error between the high noise input data and high quality target images. Further technical details can be found in the work by Lee et al. and Matsuura et al.<sup>21,22</sup> More recently, by using true UHRCT images as training target data, deep learning reconstruction algorithms that provide denoised images with enhanced spatial resolution have been developed.<sup>23</sup>

## 3. Potential imaging benefits: initial observations from phantom and patient studies

For general radiological applications, increased spatial resolution using thin slices and higher reconstruction matrixes has been shown to provide increased image quality and enhanced reader confidence by providing sharper images with less artifacts and improved detection and characterization of small details as compared to conventional CT images.<sup>24</sup>

It is conceivable that CT imaging with ultra-high resolution will allow a more comprehensive evaluation of the coronary tree through better delineation of the distal vasculature.<sup>25</sup> In Fig. 2, distal and smaller segments like diagonal and septal branches are easily observed. Additional clinical examples of cerebral and lung vasculature are provided in Fig. 3.



c) Main differences between UHR CT system and a conventional area detector system.

	UHR CT	Conventional area detector CT
Rows	160 row	320 row
Detector element size	0.25 mm x 0.25 mm	0.5 mm x 0.5 mm
Channels	1792	896
Minimal focus size X-ray tube	0.4 mm x 0.5 mm	0.9 x 0.8 mm
Matrix	512 x 512, 1024 x 1024, 2048 x 2048	512 x 512
Other hardware changes	<ul style="list-style-type: none"> <li>Redesigned gantry and couch to offer greater stability and reduce vibration to half of the level of a conventional scanner</li> <li>Redesigned DAS to reduce image noise</li> <li>Optically isolated detector elements and ultra-thin interseptal gaps obtained with new cutting techniques, resulting in a substantial increase in light-sensitive area relative to conventional CT</li> </ul>	

**Fig. 1. Comparison of a dedicated UHRCT and a conventional high-end CT scanner.** Panel (a): In the UHRCT system (Aquilion Precision), the size of the detector elements at the isocenter is 0.25 x 0.25 mm and the detector has 1792 channels in 160 rows. The minimum focus size of the x-ray tube is 0.4 x 0.5 mm. Panel (b): In a conventional high-end wide area detector CT (Aquilion ONE), the size of the detector elements at the isocenter is 0.5 x 0.5 mm and the detector has 896 channels in 320 rows. The minimum focus size of the x-ray tube is 0.9 x 0.8 mm. Panel (c): Table providing an overview of the major changes including in hardware design specifically for UHR CT as compared to conventional area detector CT. Panels (a) and (b) are reprinted with permission from Hata A. et al.<sup>17</sup>

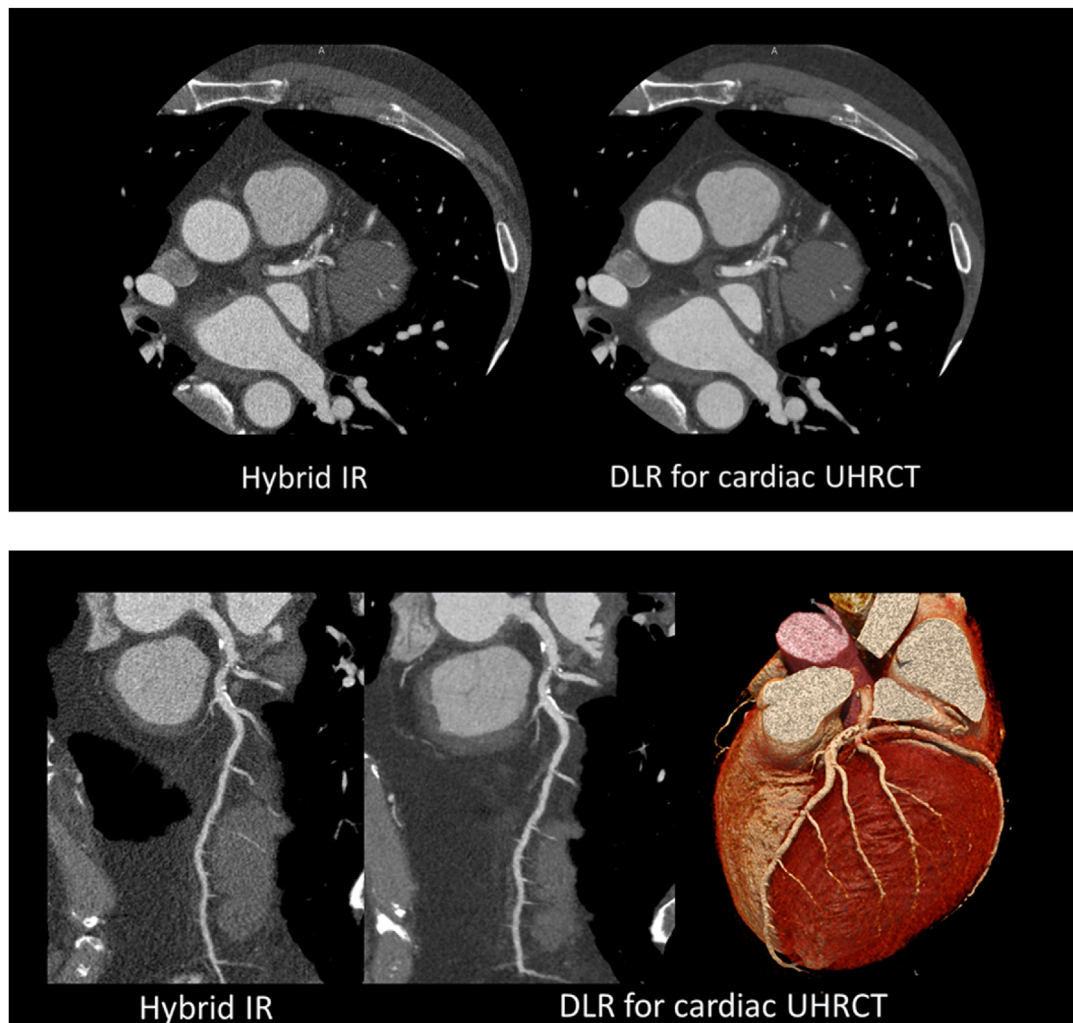


**Fig. 2.** Clinical example of UHRCT image data with deep learning-based reconstruction (DLR). Upper panel shows axial images reconstructed with hybrid iterative reconstruction (hybrid IR, no deep learning component), left image; image noise: 55 HU) and dedicated deep learning-based reconstruction for cardiac UHRCT (DLR, right image; image noise: 21 HU). Lower panel shows curved multiplanar reconstructions (MPR) of the left anterior descending coronary artery with hybrid IR (left) and DLR (middle) and a corresponding photorealistic 3D rendering image (right). Imaging using high-resolution mode is typically associated with increased noise levels.<sup>33,40</sup> While not yet available in most UHRCT publications so far, deep learning-based reconstruction has recently been introduced providing considerable noise reduction and allowing to maintain high image quality even in patients with high body mass index.

Superior detectability and visualization of small arteries ranging from intracranial microvessels to small visceral arteries have been demonstrated.<sup>26–30</sup> While conceptually attractive, visualization of the more challenging distal coronary vasculature has not yet been systematically explored.

Sharper images in combination with a reduction of partial volume effect and blooming artifacts may enable more precise grading of stenosis degree and extend the evaluation to segments with stents or extensive calcifications. The impact of ultra-high spatial resolution, obtained with either prototype PCCT or UHRCT systems, on coronary stent imaging has been evaluated in *in vitro* models.<sup>31–33</sup> Mannil et al. using a coronary vessel phantom with 18 different coronary stents of varying materials and strut thicknesses, compared images obtained with a prototype PCCT system ( $48 \times 0.25$  mm) with those from a commercially available DSCT system ( $2 \times 64 \times 0.6$  mm).<sup>32</sup> Symons et al. built on to this experience by assessing a wider range of stent diameters, including also stents with diameters  $<3.0$  mm in the phantom model.<sup>33</sup> Coronary stent lumen visibility was compared among 4 imaging and reconstruction modes. Three modes were obtained with PCCT, including PCCT-HR<sub>0.25</sub>: scanning in UHR mode with an acquired detector pixel size of  $0.25 \times 0.25$  mm<sup>2</sup> and reconstructed image voxel size of  $0.25 \times 0.25 \times 0.5$  mm<sup>3</sup>,

PCCT-HR<sub>0.5</sub>: scanning in UHR mode (acquired detector pixel size of  $0.25 \times 0.25$  mm<sup>2</sup>) but reconstructed with thicker slices (image voxel size of  $0.5 \times 0.5 \times 0.5$  mm<sup>3</sup>), and PCCT-standard resolution: PCCT scanning in standard resolution mode with acquired detector pixel size of  $0.5 \times 0.5$  mm<sup>2</sup> and reconstructed image voxel size  $0.5 \times 0.5 \times 0.5$  mm<sup>3</sup>. For comparison with conventional CT, dose-matched imaging with also performed a high-end 3rd generation dual source CT scanner with an acquired detector pixel size of  $0.5 \times 0.6$  mm<sup>2</sup> and reconstructed image voxel size of  $0.5 \times 0.5 \times 0.6$  mm<sup>3</sup>. Stent lumen visibility was significantly higher for the UHR mode with both acquisition and reconstruction in UHR. In contrast, stent lumen visibility was significantly lower for all other modes without any difference from conventional CT, suggesting that the benefits of enhanced stent visibility are primarily attributable to the resolution effect and not of other benefits of photon-counting. Similarly, using a different PCCT prototype with a  $9 \times 0.274$  mm collimation and pixel size of  $0.274 \times 0.274$  mm<sup>2</sup> at isocenter, Sigovan et al. showed better visualization of the intra-stent lumen as well as sharper delineation of the stent mesh as compared to commercially available dual-energy and conventional CT systems.<sup>34</sup>

The impact of increased spatial resolution on coronary calcium scoring was investigated by Fukumoto et al. who assessed the difference in

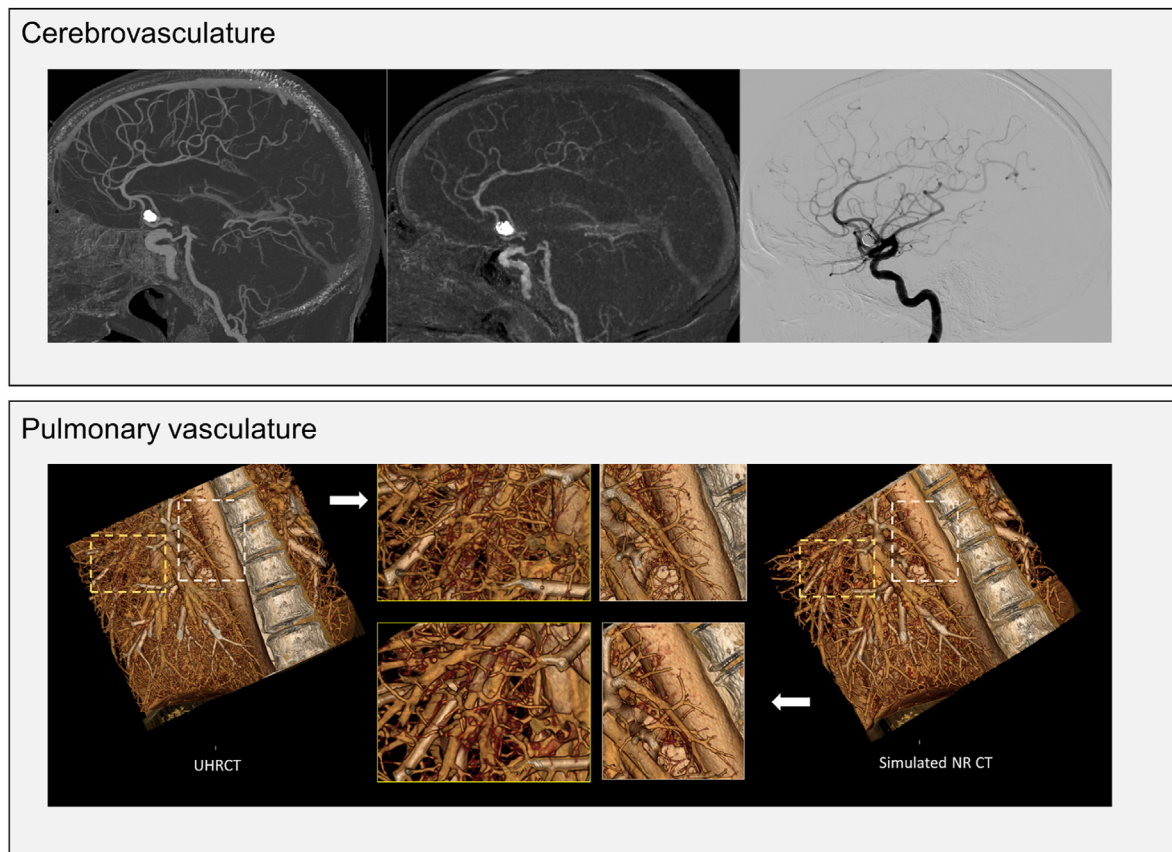


**Fig. 3. Improved visualization of the cerebrovasculature and pulmonary vasculature with UHRCT.** Upper panel: Substantially greater detail using UHRCT (left image) is visible as compared to conventional CT angiography (middle image). Invasive correlation provided on the right. Reprinted with permission.<sup>29</sup> Lower panel: Detailed visualization of the pulmonary vasculature using UHRCT (left image) as compared to simulated normal resolution CT angiography (simulated NR CT, right image). To create the synthesized normal resolution images, a dedicated raw projection data based algorithm was used to generate normal resolution images from UHR acquisitions.<sup>59</sup>

coronary artery calcium scores when scanning a coronary calcium calibration phantom and five human cadavers in either conventional (NR) and SHR mode using a commercially available UHRCT system.<sup>35</sup> Their evaluation showed that small calcifications were more accurately detected on SHR images than NR images. Mean error values were significantly lower on SHR images (14.0%) as compared to NR (20.1%,  $p = 0.01$ ). Also, inspection of the profile curves of the calcifications on the phantom images showed that blooming artifacts were reduced on UHRCT scans acquired with SHR mode as compared to NR scans. More recently, additional evidence supporting the increased coronary artery calcium detectability and more accurate calcium scoring with increased spatial resolution were reported by van der Werf et al. who compared a prototype PCCT system to a conventional CT using a static anthropomorphic phantom model.<sup>36</sup> To simulate different patient sizes, scanning was performed with and without a fat tissue-equivalent extension ring. In their investigation, increased spatial resolution allowed 34% and 4% higher detectability of calcium for the small and large phantom, respectively. These observations suggest that increased spatial resolution may allow better recognition of small calcifications as well as provide more accurate calcium scores. Recently, Yamada et al. performed a phantom comparison between a  $64 \times 0.625$  mm system and a  $32 \times 0.3125$  mm system to evaluate the impact of 2-fold spatial resolution on stenosis grading.<sup>37</sup> The authors observed that in case of non-calcified lesions, imaging with increased spatial resolution resulted in estimated stenosis severities that were not significantly different from true values, whereas imaging with conventional resolution resulted in underestimation of lesions. Both systems systematically overestimated calcified lesions although values obtained with higher spatial resolution resembled true values more closely.

So far, a large proportion of research exploring the potential value of high spatial resolution for coronary imaging has been performed using *in vitro* or *in vivo* animal models owing to the preclinical stage of most of the available PCCT technology. Clinical data are emerging with the UHRCT system. The first clinical observations were reported by Motoyama et al. using a prototype UHRCT system.<sup>38</sup> Calcifications on UHRCT were smaller and had fewer artifacts than on conventional CT, resulting in a substantial reduction of calcified lesions classified as having  $\geq 50\%$  stenosis. Additionally, stents nondiagnostic on standard resolution CT were interpretable using UHRCT. Quantitative assessment based on the average attenuation profile through the stent in the axial plane confirmed significantly larger stent lumen as well as significantly thinner stent struts on UHRCT as compared to standard resolution CT. Overall, the majority of stents with a diameter  $\geq 2.5$  mm could be evaluated by UHRCT, although interpretation of stents with a diameter of 2.25 mm or smaller remained challenging in this initial report.

Initial data on the diagnostic accuracy of coronary angiography with dedicated UHRCT systems as compared to ICA are emerging but remain scarce (Table 1).<sup>38–40</sup> Two clinical studies were performed using a prototype system,<sup>38,39</sup> whereas one study used a commercially available system.<sup>40</sup> Motoyama et al. reported high sensitivity and specificity of 100% and 80%, respectively, to detect severe stenosis on ICA on a patient basis in 59 patients with a median calcium score of 171. Takagi et al. studying 38 patients, found on a patient basis a similar sensitivity (100%) yet somewhat lower specificity (67%). More recently, preliminary experience from 15 patients enrolled in an ongoing study of high-risk patients with established, severe CAD as well as very high calcium scores (mean CACS score 1205 ranging from 249 to 2780) has been

**Table 1**  
Diagnostic accuracy of CT angiography with UHRCT to detect significant coronary stenosis.

	Motoyama et al. <sup>38</sup>	Takagi et al. <sup>39</sup>	Latina et al. <sup>40</sup>
<i>Study characteristics</i>			
N	59	38	15
System	Prototype	Prototype	Commercial
Obesity (BMI >30 kg/m <sup>2</sup> )	0	4 (11%)	9 (60%)
Heart rate (bpm)	All subjects <65	Average 57 ± 3	56 ± 6
Significant stenosis on invasive coronary angiography (patient level)	75% (significant stenosis defined as ≥75% luminal narrowing)	84% (significant stenosis defined as ≥50% luminal narrowing)	33% (significant stenosis defined as ≥70% luminal narrowing)
Extent of calcium	Median CACS 171 (IQR 49–503)	Median CACS 250 (range 3–1140)	Mean CACS 1205 (range 249–2780)
<i>Patient level</i>			
Sensitivity	100%	100%	100%
Specificity	80%	67%	100%
PPV	93.6%	94%	100%
NPV	100%	100%	100%
<i>Vessel level</i>			
Sensitivity		96%	86%
Specificity		81%	88%
PPV		80%	70%
NPV		88%	95%
<i>Segment level</i>			
Sensitivity	100%	95%	
Specificity	95.8%	96%	
PPV	79.5%	79%	
NPV	100%	99%	

Abbreviations: CACS: coronary artery calcium score, IQR: interquartile range, NPV: negative predictive value, PPV: positive predictive value.

described.<sup>40</sup> Despite high noise levels (advanced deep learning reconstruction was not yet available at the time of publication) in the setting of a mostly obese patient population (9 (60%) patients with a BMI>30

kg/m<sup>2</sup>), diagnostic confidence was good with all studies deemed fully interpretable. Average image quality and diagnostic confidence scores, ranked on a scale of 1–5, were 4.1 ± 0.8 and 4.3 ± 0.9, respectively. Comparison with ICA resulted in a sensitivity of 86% and specificity of 88%. Importantly, UHRCT was shown to be able to rule out obstructive disease despite severely elevated calcium scores. Clinical examples of patients with previous stent implantation and extensive calcium from this cohort are provided in Figs. 4 and 5, respectively.

#### 4. Opportunities for clinical application and future avenues for research

##### 4.1. Can UHRCT further reduce the number of diagnostic invasive evaluations?

During the past few years, CT angiography has established itself as the first-line diagnostic test for patients presenting with suspected CAD, a strategy supported by several large trials, such as the SCOT-HEART<sup>41</sup> and CONSERVE<sup>42</sup> trials, and integrated into the major societal guidelines.<sup>1,2</sup> As compared to conventional pathways to select candidates for ICA, application of CT has been shown to increase the diagnostic yield of ICA substantially<sup>42,43</sup> and avoid unnecessary invasive procedures in a large percentage of patients. In the CONSERVE trial, a CT angiography-guided strategy of selective rather than direct referral to ICA was shown to be safe and could avoid almost 4 out of 5 invasive procedures while significantly improving the yield of obstructive CAD.<sup>42</sup> Importantly, using CT to select candidates for invasive angiography was associated with a significant cost reduction of 57%.

Although CT angiography has become a class I recommendation for diagnosing CAD in symptomatic patients, several restrictions remain.<sup>2</sup> Overestimation of the degree of stenosis, particularly in the presence of calcification, remains a known limitation of CT angiography.<sup>5</sup> Current guidelines therefore point to a limited role for CT in higher risk populations with known disease and previous stent implantation. In practice

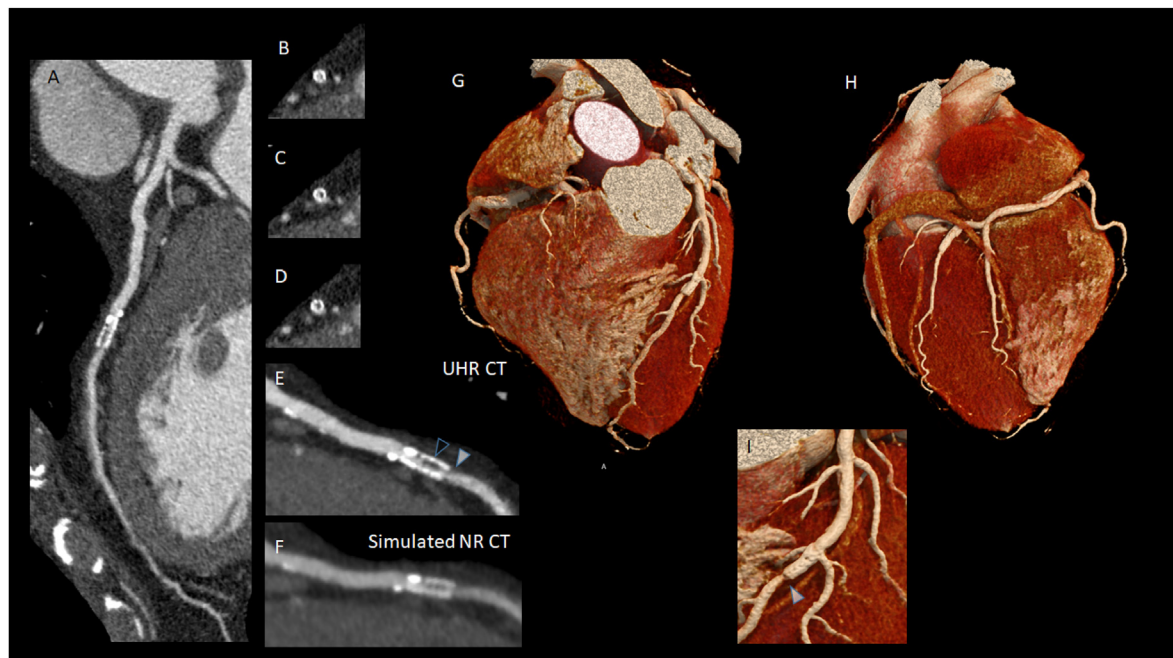


**Fig. 4. Clinical example of a patient with previous stent implantation.** On the curved multiplanar reconstructions (A, E) and cross-sectional images (B, C, D) of the left anterior descending coronary artery, neo-intimal hyperplasia in the distal portion of the stent as well as plaque formation around its distal edge can be distinguished despite the small diameter of the stent. Such detail is substantially less visible on the simulated normal resolution image (F). On the photorealistic 3D rendered images (G, H, I) detailed imaging of the coronary vasculature can be appreciated, including the luminal narrowing at the distal stent edge (I, arrowhead). Imaging was performed in SHR mode (0.25 mm in-plane and longitudinal direction), whereas a validated raw projection data based algorithm was used to generate the normal resolution image (as if acquired with 0.5 mm in-plane and longitudinal direction) from UHR acquisitions.<sup>59</sup>

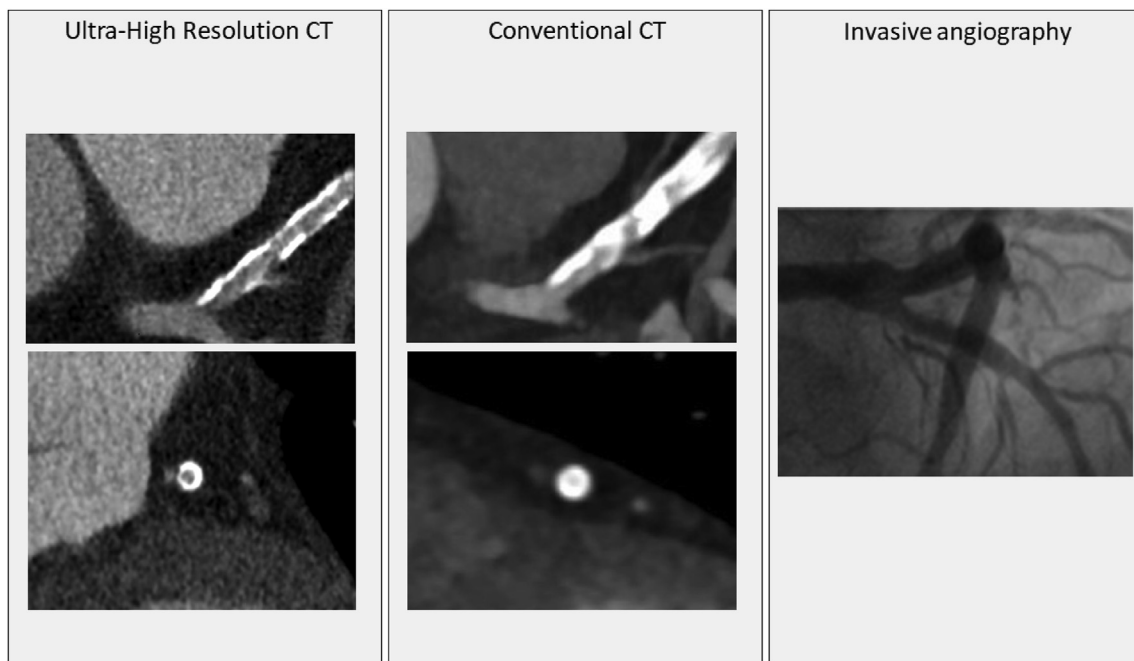


**Fig. 5. Comparison between UHRCT and conventional CT in a patient with a calcium score over 2000.** On UHRCT, the presence of significant stenosis in the proximal left anterior descending coronary artery could be ruled out despite the presence of extensive calcifications. In contrast, significant lesions could not be ruled out on conventional CT due to the substantial blooming artifacts obscuring the lumen. Invasive coronary angiography confirmed the absence of significant stenosis.

nonetheless, CT is still used to evaluate some of these patients, particularly those who should not undergo or refuse repeated invasive procedures. In addition, given the COVID-19 outbreak, diagnostic pathways that reduce potential exposure of both patients and healthcare workers to infectious diseases have rapidly become preferential, providing further arguments in support of extended usage of CT angiography beyond its traditional use even towards patients with suspected acute coronary syndrome at intermediate risk.<sup>44</sup>

Given its availability and ease of use, UHRCT coronary angiography could be beneficial to the significant population of patients with prior history of advanced CAD including those after percutaneous coronary intervention (PCI). This would extend the routine use of CT angiography to the wider, non-selected population of patients with symptomatic ischemic heart disease. The addition of functional testing has been advocated to partially overcome the limitations of sub-standard diagnostic CT angiograms. However, in the ideal situation, a large proportion of patients would be appropriately managed based on a high-quality CT angiogram alone, with selective use of functional assessment. UHRCT scanning may theoretically offer an important step in this direction. As discussed, initial explorations have indicated that the two to three-fold increase in spatial resolution offered by UHRCT translates into more accurate quantification of percent stenosis.<sup>39</sup> A significant reduction in false positive segments may have implications for downstream testing and may further reduce the need for either additional functional evaluations such as with CT-derived fractional flow reserve or invasive angiography since both have limited clinical value in the absence of significant stenosis.<sup>45</sup> Moreover, the ability to assess patients with calcifications and previous stents may extend the indications for CT angiography instead of invasive imaging methods beyond the current low to intermediate likelihood patients to higher risk or elderly patients with suspected advanced disease. In our experience, such patients represent around 25%–30% of patients that are referred for imaging in a tertiary center.<sup>5</sup>

#### 4.2. Can CT improve (shared) clinical decision making?

Already current CT systems allow to avoid diagnostic ICA in many patients. As described above, UHRCT opens the possibility to extent these

benefits to high-risk patient groups that present with more advanced disease (such as more extensive calcifications or smaller vessels) and/or previous revascularization (including stent placement). In practice, the shift towards an initial completely non-invasive diagnostic work-up even in potential candidates for revascularization could offer multiple attractive advantages. First, there is increasing awareness that separating the diagnostic phase from the therapeutic phase could improve overall clinical decision making in several ways. For example, in a recent investigation of the informed consent process for revascularization, over 40% of patients admitted not to fully understand or remember the information provided to them.<sup>46</sup> The study also revealed that more than half of patients mistakenly believed that the specific coronary interventional procedure was curative. More recently, the results of the ISCHEMIA trial have demonstrated that revascularization by coronary artery bypass grafting (CABG) or PCI can improve symptoms and quality of life, but does not alter the likelihood of major clinical cardiovascular complications including non-fatal myocardial infarction, stroke and cardiac death.<sup>47</sup>

Accordingly, there is a strong need to redesign the patient pathway to allow protected time for physicians to fully discuss the risk and benefits of the different treatment options before any invasive procedure is initiated. Such engagement will allow for greater consideration to available treatment options before reaching a shared decision. In fact, a fully non-invasive diagnostic strategy prior to intervention may allow more time to examine the potential benefits of an initial non-invasive management strategy with focus on optimal medical therapy (OMT), rather than immediate PCI once obstructive disease is observed during invasive evaluation.<sup>47</sup> Given the increasing need to constrain healthcare expenditures, restricted use of invasive procedures may also be preferential from a cost-efficiency perspective as a strategy of routinely PCI is consistently associated with greater costs as compared to OMT.<sup>48,49</sup> Evidence for an initial non-invasive diagnostic approach can be gleaned from the aforementioned CONSERVE trial<sup>42</sup> amongst others. As compared to CT guided referral, direct referral to invasive angiography was associated with an almost 40% increase in coronary revascularization rates, yet without any evidence of clinical benefit with rates of event-free survival as well as freedom of angina being identical for both

strategies at follow-up.<sup>42</sup> A streamlined evaluation and management algorithm with greater emphasis towards preventative care based on medical management and restricting invasive procedures to selected patients has recently been put forward by Ferraro et al.<sup>48</sup> UHRCT may be uniquely positioned to facilitate this change in clinical practice patterns.

#### 4.3. Can UHRCT assist in pre-procedural intervention planning?

In those patients in whom revascularization remains preferential, having dedicated time for multi-disciplinary team discussion, if applicable clinically, could lead to a more careful selection of revascularization method. In this regard, Serruys and colleagues suggested that in the future, decisions between PCI and CABG could be based on detailed images obtained with CT angiography.<sup>50</sup> In their landmark study, two separate heart teams were randomized to make treatment decisions between CABG and PCI using either CT or ICA, while blinded to all other imaging studies.<sup>51</sup> Each heart team calculated the anatomical SYNTAX score based solely on their allocated imaging modality. Subsequently, they integrated the clinical information to compute the SYNTAX Score II risk prediction model, providing a treatment recommendation of CABG, PCI, or equipoise between CABG and PCI. The authors found that the agreement concerning treatment decision between CT angiography and ICA was high, Cohen's kappa 0.82, 95% confidence interval 0.74–0.91. Moreover, the study heart teams agreed on the selection of specific coronary segments for revascularization in 80% of the cases.

CT angiography provides information beyond the mere detection of significant stenosis. Visualization and characterization of plaque burden as well as individual lesion characteristics can be applied to assess technical feasibility, consider different approaches to optimize revascularization strategy and improve success rates.<sup>52,53</sup> The ability to determine the likelihood of anatomic complete revascularization non-invasively may become an important advantage of CT, while the images could also be increasingly used for procedural guidance. For such far more personalized approach to become clinical reality, superb level of detail is mandatory. Current CT technology still lacks sufficient spatial resolution as reflected for instance by the frequent overestimation of CT-based SYNTAX scores due to calcifications.<sup>51</sup> More accurate non-invasive characterization of anatomy through increased spatial resolution could mitigate these hurdles.

#### 4.4. Can UHRCT improve monitoring of anti-atherosclerotic therapies and microvascular disease in the heart and other organ systems?

Novel therapies to reduce plaque formation over and above the effect of statins are occupying center stage in cardiovascular research. Behind most of such developments plaque reduction and/or stabilization was assessed by ICA with intravascular ultrasound or optical coherence tomography (OCT). The invasive nature has represented an important limitation to drug development in coronary vascular disease. The ability of CT angiography to quantify atherosclerotic plaque size and characterize its morphologic features including calcified and non-calcified components makes CT an ideal tool to support future investigational testing of therapeutic interventions.<sup>54,55</sup> In this context, CT imaging with enhanced resolution is superior to any other non-invasive modality. With conventional CT, accurate plaque quantification remains challenging with considerable variation in results reported between different observers as well as between expert observer and automated tools. Higher-resolution images may reduce variability between observers<sup>56</sup> and facilitate automated contour recognition tools. Accordingly, efforts towards standardization of plaque quantification, essential for clinical application, could substantially benefit from such improvements.

Given the nature of the atherosclerotic process, changes in plaque morphology and composition below the spatial resolution of conventional CT are common<sup>57</sup> and could be important clinically. UHRCT technology could allow for monitoring plaque reduction induced by cholesterol lowering therapy at the individual level, assuring patients

and physicians that the efficacy of therapy is maximized, particularly in patients with advanced or premature CAD. Possibly, CAD monitoring could be extended to atherosclerotic growth within or around stents, opening yet further windows into assessing atherosclerosis in the patient with prior PCI. The extension of such methods to the carotid arteries and other cerebral vascular structures is intuitive particularly since motion control needs are less than in the heart.<sup>26</sup>

In addition, the development of UHRCT discloses a previously unexplored landscape of vascular and other structural alterations below 400  $\mu\text{m}$ . More detailed visualization of the coronary tree including the smaller and more distal branches in combination with techniques for tissue perfusion could enable better characterization of ischemic heart disease. Because currently used technology still fails to find an appropriate underlying cause of complaints in patients with microvascular disease,<sup>58</sup> UHRCT implementation could potentially open yet unexplored windows to investigate the pathophysiology of diverse vascular processes involving the brain, the lungs and the cardiovascular system.

## 5. Summary and conclusion

The benefits that can be gleaned from the initial experiences with UHRCT are promising. Using UHRCT, more patients may receive non-invasive characterization of coronary atherosclerosis by overcoming the limitations of current CT spatial resolution in visualizing and quantifying calcified, stented or small diameter segments. UHRCT may enhance existing management pathways and guide medical anti-atherosclerotic therapies or interventional revascularization therapies. In the near term, larger investigations should confirm whether UHRCT can provide the important next leap forward in establishing cardiac CT as the preferred imaging method for the comprehensive non-invasive evaluation and management of an increasing number of increasingly complex patients and avoid invasive diagnostic evaluation. On the long term, UHRCT could contribute to pathophysiologic insights into important etiologies of morbidity and mortality worldwide.

### Relationships with industry

JDS and KLB are employees of Canon Medical Systems. JACL and AZ are supported by a research grant from Canon Medical Systems.

### Declaration of competing interest

Joanne D. Schuijff, PhD and Kirsten L. Boedeker, PhD are employees of Canon Medical Systems.

João A. C. Lima, MD and Armin Arbab-Zadeh, MD PhD MPH are supported by a research grant from Canon Medical Systems.

### References

- Gulati M, Levy PD, Mukherjee D, et al. 2021 AHA/ACC/ASE/CHEST/SAEM/SCCT/SCMR guideline for the evaluation and diagnosis of chest pain. *J Am Coll Cardiol*. 2021;78:e187–e285.
- Knuuti J, Wijns W, Saraste A, et al. 2019 ESC Guidelines for the diagnosis and management of chronic coronary syndromes. *Eur Heart J*. 2019;41:407–477.
- Kwan AC, Pourmorteza A, Stutman D, Bluemke DA, Lima JAC. Next-generation hardware advances in CT: cardiac applications. *Radiology*. 2021;298:3–17.
- Narula J, Chandrasekhar Y, Ahmadi A, et al. SCCT 2021 expert consensus document on coronary computed tomographic angiography: a report of the society of cardiovascular computed tomography. *J Cardiovasc Comput Tomogr*. 2021;15:192–217.
- Arbab-Zadeh A, Miller JM, Rochitte CE, et al. Diagnostic accuracy of computed tomography coronary angiography according to pre-test probability of coronary artery disease and severity of coronary arterial calcification. The CORE-64 (Coronary Artery Evaluation Using 64-Row Multidetector Computed Tomography Angiography) International Multicenter Study. *J Am Coll Cardiol*. 2012;59:379–387.
- Song YB, Arbab-Zadeh A, Matheson MB, et al. Contemporary discrepancies of stenosis assessment by computed tomography and invasive coronary angiography. *Circular: Cardiovasc Imag*. 2019;12.
- Willemink MJ, Persson M, Pourmorteza A, Pelc NJ, Fleischmann D. Photon-counting CT: technical principles and clinical prospects. *Radiology*. 2018;289:293–312.



8. Sandfort V, Persson M, Pourmorteza A, Noel PB, Fleischmann D, Willemink MJ. Spectral photon-counting CT in cardiovascular imaging. *J Cardiovasc Comput Tomogr*. 2021;15:218–225.
9. Leng S, Bruesewitz M, Tao S, et al. *Photon-counting Detector CT: System Design and Clinical Applications of an Emerging Technology*. vol. 39. Radiographics : a review publication of the Radiological Society of North America, Inc.; 2019:729–743.
10. Rajendran K, Petersilka M, Henning A, et al. Full field-of-view, high-resolution, photon-counting detector CT: technical assessment and initial patient experience. *Phys Med Biol*. 2021;66.
11. Rajendran K, Petersilka M, Henning A, et al. First clinical photon-counting detector CT system: technical evaluation. *Radiology*. 2021 (Press).
12. Pourmorteza A, Symons R, Henning A, Ulzheimer S, Bluemke DA. Dose efficiency of quarter-millimeter photon-counting computed tomography: first-in-human results. *Invest Radiol*. 2018;53:365–372.
13. Boccalini S, Si-Mohamed SA, Lacombe H, et al. First in-human results of computed tomography angiography for coronary stent assessment with a spectral photon counting computed tomography. *Invest Radiol*. 2021.
14. da Silva J, Grönberg F, Cederström B, et al. Resolution characterization of a silicon-based, photon-counting computed tomography prototype capable of patient scanning. *J Med Imag*. 2019;6.
15. Oostveen LJ, Boedeker KL, Brink M, Prokop M, de Lange F, Sechopoulos I. Physical evaluation of an ultra-high-resolution CT scanner. *Eur Radiol*. 2020;30:2552–2560.
16. Yanagawa M, Tsubamoto M, Satoh Y, et al. Lung adenocarcinoma at CT with 0.25-mm section thickness and a 2048 matrix: high-spatial-resolution imaging for predicting invasiveness. *Radiology*. 2020;297:462–471.
17. Hata A, Yanagawa M, Honda O, et al. Effect of matrix size on the image quality of ultra-high-resolution CT of the lung: comparison of 512 x 512, 1024 x 1024, and 2048 x 2048. *Acad Radiol*. 2018;25:869–876.
18. Narita K, Nakamura Y, Higaki T, Akagi M, Honda Y, Awai K. Deep learning reconstruction of drip-infusion cholangiography acquired with ultra-high-resolution computed tomography. *Abdom Radiol (NY)*. 2020;45:2698–2704.
19. Urikura A, Yoshida T, Nakaya Y, Nishimaru E, Hara T, Endo M. Deep learning-based reconstruction in ultra-high-resolution computed tomography: can image noise caused by high definition detector and the miniaturization of matrix element size be improved? *Phys Med*. 2021;81:121–129.
20. Tatsugami F, Higaki T, Nakamura Y, et al. Deep learning-based image restoration algorithm for coronary CT angiography. *Eur Radiol*. 2019;29:5322–5329.
21. Lee T-C, Zhou J, Yu Z, Matej S, Metzler SD. Deep learning based adaptive filtering for projection data noise reduction in x-ray computed tomography. In: *15th International Meeting on Fully Three-Dimensional Image Reconstruction in Radiology and Nuclear Medicine*. 2019.
22. Matsuura M, Zhou J, Akino N, Yu Z. Feature-aware deep-learning reconstruction for context-sensitive X-ray computed tomography. *IEEE Trans Radiat Plasma Med Sci*. 2021;5:99–107.
23. Tatsugami F, Higaki T, Matsuura M, Taguchi H, Tsuchida S, Awai K. Improvement of spatial resolution by using super-resolution deep learning reconstruction at coronary CT angiography. In: *Presented at: Radiological Society of North America 2021 Scientific Assembly and Annual Meeting, November 28–December 2, 2021*. Chicago, IL.
24. Shanbhag SM, Schuzer JL, Steveson C, et al. Prototype ultrahigh-resolution computed tomography for chest imaging: initial human experience. *J Comput Assist Tomogr*. 2019;43:805–810.
25. Morisaka H, Shimizu Y, Adachi T, et al. Effect of ultra high-resolution computed tomography and model-based iterative reconstruction on detectability of simulated submillimeter artery. *J Comput Assist Tomogr*. 2020;44:32–36.
26. Murayama K, Suzuki S, Nagata H, et al. Visualization of lenticulostriate arteries on CT angiography using ultra-high-resolution CT compared with conventional-detector CT. *AJNR Am J Neuroradiol*. 2020;41:219–223.
27. Yoshioka K, Tanaka R, Takagi H, et al. Ultra-high-resolution CT angiography of the artery of Adamkiewicz: a feasibility study. *Neuroradiology*. 2018;60:109–115.
28. Nagata H, Murayama K, Suzuki S, et al. Initial clinical experience of a prototype ultra-high-resolution CT for assessment of small intracranial arteries. *Jpn J Radiol*. 2019;37:283–291.
29. Meijer FJA, Schuijf JD, de Vries J, Boogaarts HD, van der Woude WJ, Prokop M. Ultra-high-resolution subtraction CT angiography in the follow-up of treated intracranial aneurysms. *Insights imag*. 2019;10:2.
30. Ogawa K, Onishi H, Hori M, et al. Visualization of small visceral arteries on abdominal CT angiography using ultra-high-resolution CT scanner. *Jpn J Radiol*. 2021;39:889–897.
31. Onishi H, Hori M, Ota T, et al. Phantom study of in-stent restenosis at high-spatial-resolution CT. *Radiology*. 2018;289:255–260.
32. Mannil M, Hieckthier T, von Spiczak J, et al. Photon-counting CT: high-resolution imaging of coronary stents. *Invest Radiol*. 2018;53:143–149.
33. Symons R, De Bruecker Y, Roosen J, et al. Quarter-millimeter spectral coronary stent imaging with photon-counting CT: initial experience. *J Cardiovasc Comput Tomogr*. 2018;12:509–515.
34. Sigovan M, Si-Mohamed S, Bar-Ness D, et al. Feasibility of improving vascular imaging in the presence of metallic stents using spectral photon counting CT and K-edge imaging. *Sci Rep*. 2019;9:19850.
35. Fukumoto W, Nagaoka M, Higaki T, et al. Measurement of coronary artery calcium volume using ultra-high-resolution computed tomography: a preliminary phantom and cadaver study. *Eur J Radiol Open*. 2020;7:100253.
36. van der Werf NR, Si-Mohamed S, Rodesch PA, et al. Coronary calcium scoring potential of large field-of-view spectral photon-counting CT: a phantom study. *Eur Radiol*. 2022;32:152–162.
37. Yamada M, Yamada Y, Nakahara T, et al. Accuracy of ultra-high-resolution computed tomography with a 0.3-mm detector for quantitative assessment of coronary artery stenosis grading in comparison with conventional computed tomography: a phantom study. *J Cardiovasc Comput Tomogr*. 2021.
38. Motoyama S, Ito H, Sarai M, et al. Ultra-high-resolution computed tomography angiography for assessment of coronary artery stenosis. *Circular J*. 2018;82:1844–1851.
39. Takagi H, Tanaka R, Nagata K, et al. Diagnostic performance of coronary CT angiography with ultra-high-resolution CT: comparison with invasive coronary angiography. *Eur J Radiol*. 2018;101:30–37.
40. Latina J, Shabani M, Kapoor K, et al. Ultra-high-resolution coronary CT angiography for assessment of patients with severe coronary artery calcification: initial experience. *Radiol Cardiothorac Imag*. 2021;3, e210053.
41. Newby DE, Adamson PD, Berry C, et al. Coronary CT angiography and 5-year risk of myocardial infarction. *N Engl J Med*. 2018;379:924–933.
42. Chang HJ, Lin FY, Gebow D, et al. Selective referral using ccta versus direct referral for individuals referred to invasive coronary angiography for suspected CAD: a randomized, controlled, open-label trial. *JACC Cardiovasc imag*. 2019;12:1303–1312.
43. Patel MR, Peterson ED, Dai D, et al. Low diagnostic yield of elective coronary angiography. *N Engl J Med*. 2010;362:886–895.
44. The European Society for Cardiology. *ESC Guidance for the Diagnosis and Management of CV Disease during the COVID-19 Pandemic*. 2020.
45. McNabney CG, Sellers SL, Wilson RJA, et al. Prognosis of CT-derived fractional flow reserve in the prediction of clinical outcomes. *Radiol Cardiothorac Imag*. 2019;1, e190021.
46. Astin F, Stephenson J, Probyn J, Holt J, Marshall K, Conway D. Cardiologists' and patients' views about the informed consent process and their understanding of the anticipated treatment benefits of coronary angioplasty: a survey study. *Eur J Cardiovasc Nurs*. 2020;19:260–268.
47. Maron DJ, Hochman JS, Reynolds HR, et al. Initial invasive or conservative strategy for stable coronary disease. *N Engl J Med*. 2020;382:1395–1407.
48. Ferraro R, Latina JM, Alfaddagh A, et al. Evaluation and management of patients with stable Angina: beyond the ischemia paradigm. *J Am Coll Cardiol*. 2020;76:2252–2266.
49. Weintraub WS, Boden WE, Zhang Z, et al. Cost-effectiveness of percutaneous coronary intervention in optimally treated stable coronary patients. *Circular Cardiovasc Qual Outcome*. 2008;1:12–20.
50. Serruys PW, Chichareon P, Modolo R, et al. *The SYNTAX Score on its Way Out or towards Artificial Intelligence: Part II*. EuroIntervention; 2019.
51. Collet C, Onuma Y, Andreini D, et al. Coronary computed tomography angiography for heart team decision-making in multivessel coronary artery disease. *Eur Heart J*. 2018;39:3689–3698.
52. Opolski MP, Achenbach S. CT angiography for revascularization of CTO: crossing the borders of diagnosis and treatment. *JACC Cardiovasc imag*. 2015;8:846–858.
53. Hong SJ, Kim BK, Cho I, et al. Effect of coronary CTA on chronic total occlusion percutaneous coronary intervention: a randomized trial. *JACC Cardiovasc imag*. 2021;14:1993–2004.
54. Symons R, Morris JZ, Wu CO, et al. Coronary CT angiography: variability of CT scanners and readers in measurement of plaque volume. *Radiology*. 2016;281:737–748.
55. Henzel J, Kepka C, Kruk M, et al. High-risk coronary plaque regression after intensive lifestyle intervention in nonobstructive coronary disease. *JACC (J Am Coll Cardiol): Cardiovasc Imag*. 2021;14:1192–1202.
56. Takagi H, Fusazaki T, Orii M, et al. Interscan reproducibility of coronary plaque volume measurements using ultra-high-resolution ct. *J Cardiovasc Comput Tomogr*. 2020;14:S75–S76.
57. Sandfort V, Lima JA, Bluemke DA. Noninvasive imaging of atherosclerotic plaque progression: status of coronary computed tomography angiography. *Circular Cardiovasc imag*. 2015;8, e003316.
58. Bairey Merz CN, Pepine CJ, Walsh MN, Fleg JL. Ischemia and No obstructive coronary artery disease (INOCA): developing evidence-based therapies and research agenda for the next decade. *Circulation*. 2017;135:1075–1092.
59. Hernandez AM, Shin DW, Abbey CK, et al. Validation of synthesized normal-resolution image data generated from high-resolution acquisitions on a commercial CT scanner. *Med Phys*. 2020;47:4775–4785.